

A subadult specimen of *Pengornis* and character evolution in Enantiornithes

HU Han^{1,2} ZHOU Zhong-He¹ Jingmai K. O'CONNOR¹

(1 Key Laboratory of Vertebrate Evolution and Human Origins of Chinese Academy of Sciences, Institute of Vertebrate Paleontology and Paleoanthropology, Chinese Academy of Sciences Beijing 100044 huhan_ivpp@163.com)

(2 University of Chinese Academy of Sciences Beijing 100049)

Abstract Previously known only from the holotype specimen, *Pengornis houi* is the largest known Early Cretaceous enantiornithine bird and important for understanding body size and character evolution in Ornithothoraces. We report on a new subadult specimen from the Lower Cretaceous Jiufotang Formation referred to *Pengornis* sp. The specimen preserves a nearly complete sternum, reminiscent of that in *Protopteryx* and the basal ornithuromorph *Archaeorhynchus*, confirming the basal position of *Pengornis* and shedding new light on the evolution of the sternum in ornithothoracines. Anatomical information suggests that despite its size, *Pengornis* was arboreal, like other enantiornithines.

Key words western Liaoning, Early Cretaceous, Jiufotang Formation, enantiornithine, *Pengornis*

Since Enantiornithes was first recognized over three decades ago (Walker, 1981), dozens of new enantiornithine taxa have been discovered from the Lower Cretaceous Jehol Group of northeastern China (Benton et al., 2008). This fossil-rich lacustrine unit consists of the lower Dabeigou Formation, exposed only in Hebei, the middle Yixian Formation, and the overlying Jiufotang Formation (Zhou et al., 2003).

Pengornis is the largest known Early Cretaceous enantiornithine bird. The holotype and only previously known specimen of *Pengornis houi* (IVPP V 15336) preserves features previously considered unique to Ornithuromorpha such as the relatively more globose humeral head and the hooked acromion process on the scapula, providing evidence for a complex pattern of character evolution in ornithuromorph and enantiornithine birds (Zhou et al., 2008). Although the holotype specimen of *P. houi* preserves a great deal of anatomical information, particularly regarding the skull, preservation obscures many anatomical details of the disarticulated forelimb and hindlimb, the thoracic and pelvic girdles are incomplete, and no plumage is preserved. Recently, a nearly complete subadult specimen (IVPP V 18632) was recovered from the Jiufotang Formation of Lingyuan, western Liaoning, very near the locality that produced the holotype of *P. houi*. Morphological comparisons between this new specimen and the holotype of *P. houi* show that the new specimen can be referred to *Pengornis*, and may

represent a new species; however, considering its subadult status, the specimen is referred to *Pengornis* sp. This specimen provides new information regarding the anatomy and ontogeny of the *Pengornis* genus, which in turn makes it possible to elucidate the phylogenetic position of this taxon in greater detail.

1 Systematic paleontology

Aves Linnaeus, 1758

Ornithothoraces Chiappe, 1995

Enantiornithes Walker, 1981

***Pengornis* Zhou et al., 2008**

Known taxa *Pengornis houi* (Zhou et al., 2008) from the Early Cretaceous Jiufotang Formation, northeastern China.

Diagnosis Large enantiornithine bird with the following unique combination of morphological characters: premaxillae entirely unfused; 9-13 dentary teeth that are small, brachyodont, and unrecurved; hooked scapular acromion (modified from Zhou et al., 2008).

***Pengornis* sp.**

Referred specimen IVPP V 18632 (Figs. 1, 2), a nearly complete articulated skeleton of a subadult individual with integument, lacking parts of the cervical and thoracic vertebral



Fig. 1 Photo of the subadult specimen of *Pengornis* sp. (IVPP V 18632)

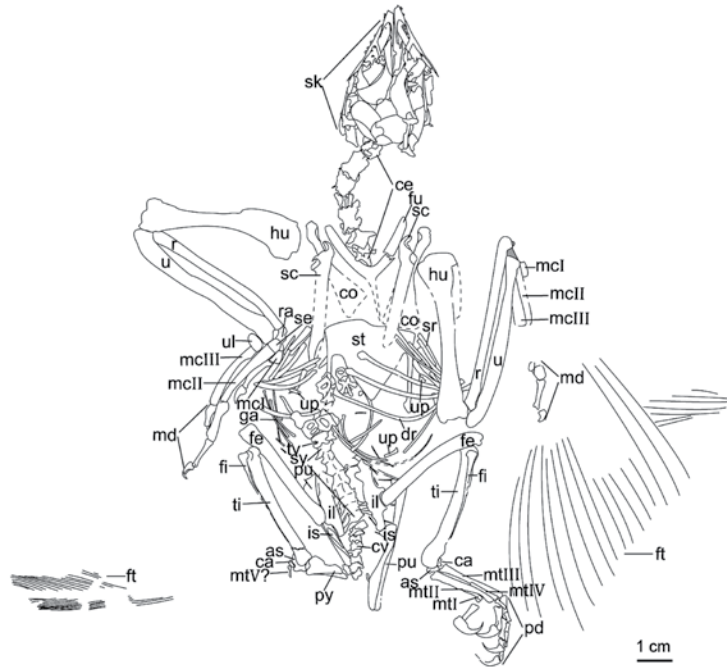


Fig. 2 Camera lucida drawing of the subadult specimen of *Pengornis* sp. (IVPP V 18632)

Abbreviations: as. astragalus 距骨; ca. calcaneum 跟骨; ce. cervical vertebrae 颈椎; co. coracoid 乌喙骨; cv. caudal vertebrae 尾椎; dr. dorsal rib 背肋; fe. femur 股骨; fi. fibula 腓骨; ft. feathers 羽毛; fu. furcula 叉骨; ga. gastralia 腹肋; hu. humerus 肱骨; il. ilium 髌骨; is. ischium 坐骨; mcl-I-III. metacarpals I-III 第一~第三掌骨; md. manual digits 指骨; mtI-V. metatarsals I-V 第一~第五跖骨; pd. pedal digits 趾骨; pu. pubis 耻骨; py. pygostyle 尾综骨; r. radius 桡骨; ra. radiale 桡腕骨; sc. scapula 肩胛骨; se. semilunate carpal 半月形腕骨; sk. skull 头骨; sr. sternal rib 胸肋; st. sternum 胸骨; sy. synsacrum 愈合荐椎; ti. tibia 胫骨; tv. thoracic vertebrae 胸椎; u. ulna 尺骨; ul. ulnare 尺腕骨; up. uncinat process 钩突

series, the distal half of the right forelimb and the distal half of the left hindlimb.

Locality and horizon Lingyuan, Chaoyang, Liaoning, China, Jiufotang Formation, Early Cretaceous (He et al., 2004).

Ontogenetic assessment the specimen is regarded as a subadult based on its smaller size relative to the holotype of *Pengornis houi* (the femur is 72.5% that of *P. houi* IVPP V 15336), the articular ends of the long bones porous and coarse, and the absence of fusion between the distal carpals and metacarpals, sacrals, and proximal tarsals and metatarsals.

2 Description

The following description is based on the anatomy of IVPP V 18632, a nearly complete, referred subadult specimen of *Pengornis*, with comparisons to the holotype of *P. houi* IVPP V 15336. Anatomical nomenclature primarily follows Baumel and Witmer (1993); English is used for osteological features while Latin is maintained for muscles.

Skull and mandibles The skull is nearly complete (Fig. 3), preserved in dorsal view (lateral view in V 15336), but the individual bones are crushed and slightly disarticulated.

The premaxillae are entirely unfused and relatively small and short as described for

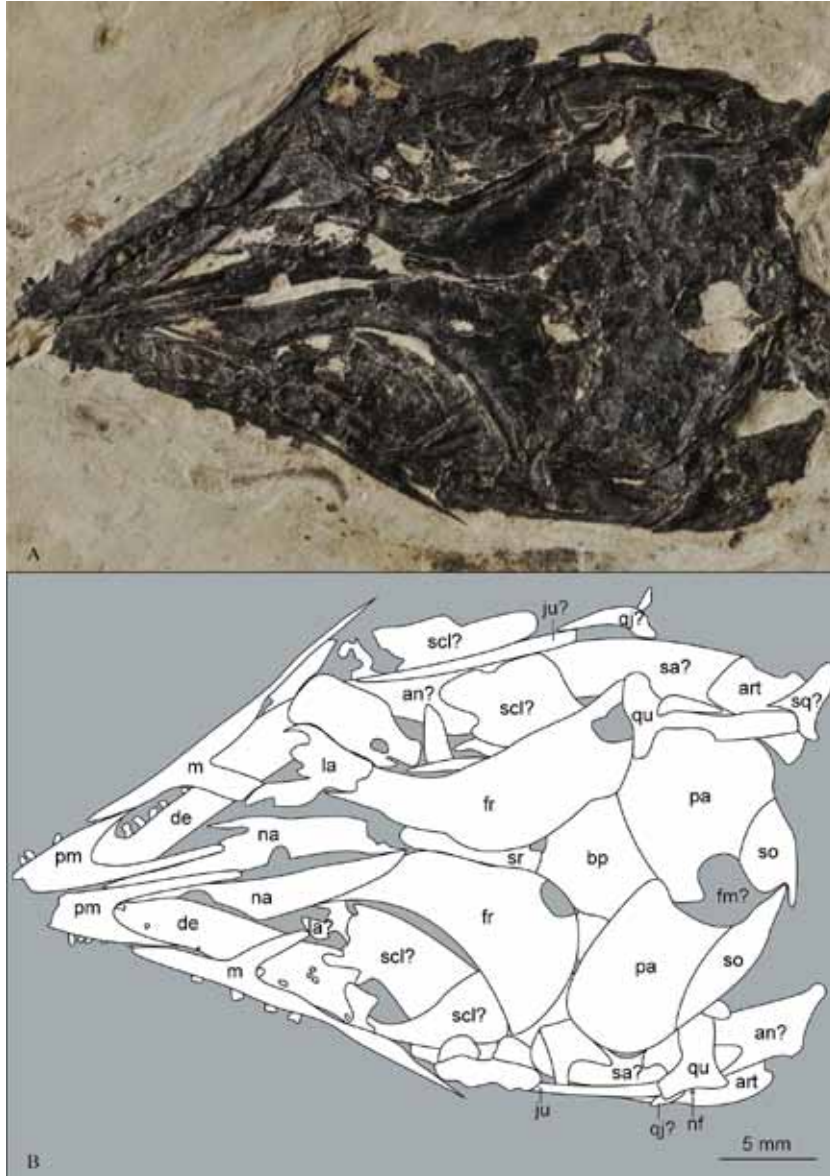


Fig. 3 Photo (A) and camera lucida drawing (B) of the skull of the subadult specimen of *Pengornis* sp. (IVPP V 18632)

Abbreviations: an. angular 隅骨; art. articular 关节骨; bp. basitemporal plate 基颞板; de. dentary 齿骨; fm. foramen magnum 枕骨大孔; fr. frontal 额骨; ju. jugal 颧骨; la. lacrimal 泪骨; m. maxilla 上颌骨; na. nasal 鼻骨; nf. nutrient foramina 营养孔; pa. parietal 顶骨; pm. premaxilla 前颌骨; qj. quadratojugal 方颧骨; qu. quadrate 方骨; sa. surangular 上隅骨; scl. sclerotic bones 巩膜骨; so. supraoccipital 上枕骨; sp. splenial 夹板骨; sq. squamosal 鳞骨; sr. sphenoid rostrum 蝶骨突

Pengornis houi V 15336 (Zhou et al., 2008). The imperforate corpus is short, only slightly longer than the tapered maxillary processes, which defines an angle of approximately 34° with the short frontal processes. The frontal processes are strap-like and end near the level of caudal margin of the external nares, similar to *Archaeopteryx*, *Cathayornis* (Martin and Zhou, 1997) and *Eoenantiornis* (Hou et al., 1999). In *Protopteryx* (Zhang and Zhou, 2000) and most other enantiornithines, the frontal process of the premaxilla is more elongate extending to the level of the lacrimal (O'Connor and Chiappe, 2011). The right premaxilla preserves three teeth, missing the first one; the left bears all four teeth. The premaxillary teeth are small and low crowned, similar to that of *P. houi* (Zhou et al., 2008), but contrasting with the more robust teeth typical of most enantiornithines, such as *Protopteryx* (Zhang and Zhou, 2000). The teeth appear smaller than in *P. houi* holotype (0.48–0.58 mm in V 18632 and 0.55–0.65 mm in *P. houi* holotype). The cranialmost premaxillary teeth are closely packed, but the poorly preserved fourth is more widely separated.

The maxilla forms about half of the facial margin in each side, and differs from the maxilla of *Pengornis houi* holotype in having more delicate nasal processes (Zhou et al., 2008). The premaxillary process tapers rostrally to articulate with the premaxilla, and the jugal process is constricted and tapers caudally. The antorbital fenestrae are not well preserved. Four teeth are preserved in the left maxilla. The teeth are slightly larger than the premaxillary teeth; they appear rectangular with flat crowns, which we suggest results from poor preservation. In *P. houi* holotype (Zhou et al., 2008), the caudal end of the maxilla bears a concave dorsal facet that articulates with the slender and ventrally curved jugal bar. The jugal is more slender in V 18632 than in *P. houi* holotype (Zhou et al., 2008). An L-shaped element caudal to the right jugal is tentatively identified as the quadratojugal; the jugal ramus is approximately twice the length of the ascending ramus.

The nasals are long, unfused, and fairly narrow (the width-to-length ratio is 0.12 rather than 0.18 in *P. houi* holotype V 15336); they contact the premaxillae medially along the rostral third of their length. The caudal margins are not well preserved. The cranial margin of each nasal is incised by a concave surface, defined by the long, tapered premaxillary process and the short, sharply tapered maxillary process; the latter is not preserved in *P. houi* holotype (O'Connor and Chiappe, 2011).

The orbital and postorbital regions are poorly preserved in V 18632 compared to *Pengornis houi* V 15336 (Zhou et al., 2008). In *P. houi* V 15336, the dorsal surface of the lacrimal is concave where it contacts the nasal, defining an accessory fenestra; it articulates with the maxilla via a “U”-shaped facet in the dorsal process of the maxilla (Zhou et al., 2008). Neither of these features can be confirmed in the new specimen. The lacrimal appears to be ‘Y’ shaped; the ventral branch is straight with a groove in the lateral surface, as in *P. houi* V 15336 (Zhou et al., 2008). The postorbital, like that present in *P. houi* V 15336 (Zhou et al., 2008), cannot be identified in V 18632. A few sclerotic bones are preserved in the orbital region on each side of the skull, but the exact number of scleral ossicles cannot be counted in V 18632.

The frontals are entirely unfused in V 18632, and slightly disarticulated due to dorsoventral compression. The frontals are tapered rostrally, and expanded caudally, as in other ornithothoracines. Each frontal articulates rostrally with the caudal margin of the nasal; the right is slightly disarticulated and preserved in articulation with the lacrimal, suggesting these bones may also contact. The lateral margin of the frontals is ventrally concave and indicates the presence of a large orbit. Caudally, the frontals are unfused to the parietals. The parietals are quadrangular and unfused to each other. The space between the parietals and the supraoccipitals is interpreted as due to disarticulation.

The quadrate is preserved in both *Pengornis houi* holotype and the new specimen. The orbital process is not preserved in either; the otic process is long and single-headed as in *Archaeopteryx* and enantiornithines (*Cathayornis* (Martin and Zhou, 1997), *Protopteryx* (Zhang and Zhou, 2000), *Eocathayornis* (Zhou, 2002), *Shenqiornis* (Wang et al., 2010) and *Rapaxavis* (O'Connor et al., 2011)). In lateral view the quadrate in *P. houi* V 15336 is slightly bowed, as in *Rapaxavis* (O'Connor et al., 2011), but in V 18632 it is preserved in cranial view and appears nearly straight. In V 18632, the mandibular articulation surface of the quadrate is formed by two transversely aligned condyles that are equivalent in size; the medial condyle is twice the length of the lateral condyle in *Shenqiornis* (Wang et al., 2010) and *Rapaxavis* (O'Connor et al., 2011).

The mandibular bones are largely covered by the cranial elements in V 18632. Dentary teeth are small and numerous, similar to *P. houi*, and different from other enantiornithines. In V 18632, approximately nine teeth are present in the left dentary, and five teeth in the right dentary; in *P. houi* V 15336 approximately thirteen teeth are present in the exposed left dentary. The teeth in *Pengornis* (both in V 15336 and in V 18632) are smaller than most other enantiornithines, except *Longirostravis* (0.45–0.5 mm). The teeth of both V 18632 and V 15336 are nearly straight, lacking the caudally recurved crowns of many enantiornithines (O'Connor and Chiappe, 2011).

Vertebral column and ribs The vertebral series in V 18632 is poorly preserved compared to that in *Pengornis houi* holotype; the caudal cervical vertebrae and most of the thoracic vertebrae are not preserved, but the synsacrum is fairly complete and some free caudal vertebrae are preserved.

The seven cervical vertebrae visible in V 18632 are articulated and exposed in dorsal view; they are preserved extending from the base of the skull to the interclavicular symphysis of the furcula. They are all strongly dorsoventrally compressed. The caudal portion of the cervical series is not preserved, so the total number of cervical vertebrae cannot be determined. The most proximal visible cervical is largely obscured by the supraoccipitals, and it is uncertain whether this vertebra is the atlas, the axis, or a postaxial cervical. The spinous processes are reduced as in other enantiornithines (Chiappe and Walker, 2002). The postzygapophyses are robust and project caudally. The shorter and more slender prezygapophyses project cranially in the proximal visible six cervical, but project laterally and are expanded distally in the seventh

cervical. In the holotype of *P. houi*, the cranial cervical centra are heterocoelous and the caudal vertebrae are amphicoelous (Zhou et al., 2008), as reported in *Eocathayornis* (Zhou, 2002). The cervical vertebrae in V 18632 are mostly articulated revealing only limited information regarding the nature of the articular surfaces; only the cranial articular surface of the sixth cervical is visible and it is heterocoelous — mediolaterally concave and slightly dorsoventrally convex.

Six thoracic vertebrae are preserved in V 18632. Two of these are relatively complete, preserved near the sternum; four crushed vertebrae lie proximal to the synsacrum. The length-to-width ratio of each centrum is about 1.5, as in *P. houi* V 15336. The spinous processes are high, as in *Shenqiornis* (Wang et al., 2010) and *Iberomesornis* (Sanz and Bonaparte, 1992). The amphicoelous thoracic vertebrae bear deep lateral excavations and cranially positioned parapophyses, as in *P. houi* and other enantiornithines (Zhou et al., 2008; Chiappe and Walker, 2002).

The number of vertebrae in the synsacrum was estimated to be seven in *Pengornis houi* (Zhou et al., 2008), but we count eight in V 18632. We believe the difference is due to overlap of the cranialmost sacral by other bones (e.g., pelvis) in the holotype of *P. houi*. The presence of eight sacrals is typical for Enantiornithes, as exemplified by *Sinornis* (Serenó et al., 2002), *Iberomesornis* (Serenó, 2000), *Longipteryx* (Zhang et al., 2001), *Vescornis* (Zhang et al., 2004) and *Rapaxavis* (O'Connor et al., 2011). The synsacrum in V 18632 is longer than the ilia (Table 1). The sacrals are fully fused in *P. houi* (Zhou et al., 2008), but this is not the case in the subadult V 18632. The transverse processes, well preserved in *P. houi* holotype, are poorly preserved in V 18632. In *P. houi*, the transverse processes are enlarged and expanded distally, so those of the last three sacrals contact each other (Zhou et al., 2008). In V 18632 the transverse processes of the last three sacrals remain separate from each other, although they are all in contact with the ilia. The spinous processes are fused to form a contiguous crest, which diminishes caudally.

Eight badly crushed free caudal vertebrae are preserved in articulation in V 18632. At least four spinous processes can be identified in the pygostyle, indicating fusion was incomplete. The total length of the pygostyle in V 18632 is 9.2 mm, which is shorter than the combined length of the free caudals (15.3 mm). The cranially located dorsal fork, which is a characteristic of enantiornithines, is not obvious in the new specimen. The distal end forms a fork and the base of the pygostyle has a laminar process that projects ventrally.

The ribs are disarticulated from both the vertebrae and the sternum in the new specimen. The dorsal ribs are long and curved; a few fragments potentially represent unfused uncinat processes. The sternal ribs on either side of the sternum are preserved parallel to each other, but not in articulation with the sternum. They are half the length of the dorsal ribs and more robust. Several slender disarticulated elements near the caudal thoracic vertebrae are interpreted as gastralia.

Table 1 Measurements of the subadult specimen of *Pengornis* sp. (IVPP V 18632) (mm)

Element	Measurement	Element	Measurement
Skull length	39.7	Major phalanx-3 length (left)	4.5
Synsacrum length	22.1	Minor phalanx-1 length (left)	6.3
Synsacrum maximum width	9.9*	Minor phalanx-2 length (left)	1.0
Combined length of free caudals	15.3	Ilium length (right)	21.1*
Pygostyle	9.2	Pubis length (right)	38.4*
Sternum length	22.8*	Femur length (right)	34.8
Sternum width	26.7*	Tibia length (right)	37.7*
Sternum, lateral trabecula length (right)	17.8	Fibula length (right)	26.5*
Scapula length (left)	34.9	Metatarsal I length (right)	6.6*
Furcula proximal width	23.5	Metatarsal II length (right)	19.1*
Humerus length (left)	45.7	Metatarsal III length (right)	19.7*
Humerus, midshaft width (left)	4.5	Pedal phalanx I-1 length (right)	5.8*
Ulna length (left)	49.0	Pedal phalanx I-2 length (right)	8.2*
Ulna, midshaft width (left)	3.5	Pedal phalanx II-2 length (right)	6.1
Radius length (left)	45.5	Pedal phalanx II-3 length (right)	7.0*
Radius, midshaft width (left)	2.7	Pedal phalanx III-1 length (right)	6.8
Carpometacarpus length (left)	23.8	Pedal phalanx III-2 length (right)	6.0
Alular metacarpal length (left)	4.2	Pedal phalanx III-3 length (right)	6.4
Major metacarpal length (left)	20.1	Pedal phalanx III-4 length (right)	5.2
Minor metacarpal length (left)	19.7	Pedal phalanx IV-1 length (right)	3.8
Alular phalanx-1 length (left)	10.7	Pedal phalanx IV-2 length (right)	3.1
Alular phalanx-2 length (left)	5.5	Pedal phalanx IV-3 length (right)	2.8
Major phalanx-1 length (left)	12.5	Pedal phalanx IV-4 length (right)	4.4
Major phalanx-2 length (left)	8.8	Pedal phalanx IV-5 length (right)	6.5

* Preserved length.

Sternum The sternum is not preserved in *Pengornis houi* V 15336, but is nearly completely preserved in V 18632 in dorsal view. The morphology of the sternum is unique, but resembles the condition in *Protopteryx* (Zhang and Zhou, 2000). This bone is short and broad as in other enantiornithines with the maximum width measuring approximately 1.2 times the maximum length (the ratio is 1.06 in *Protopteryx* (Zhang and Zhou, 2000) and 1.1 in *Longipteryx* (Zhang et al., 2001)). The rostral margin is slightly broken but it appears to be minimally vaulted, as in *Shanweinia* (O'Connor et al., 2009). The preserved cranial lateral corner forms an obtuse angle of approximately 105°. The lateral margin of the sternum is straight, as in some other enantiornithines (e.g. *Protopteryx* (Zhang and Zhou,

2000), *Dapingfangornis* (Li et al., 2006), and *Rapaxavis* (O'Connor et al., 2011)). The paired slender lateral trabeculae form approximately 76% length of the lateral margin of the sternum, which is greater than in most enantiornithines (e.g. approximately 59% in *Rapaxavis*, 56% in *Longipteryx*). The distal tips are slightly expanded, similar to *Protopteryx* (Zhang and Zhou, 2000), lacking the large expansions in other enantiornithines (e.g. *Longipteryx*, *Concornis*, *Rapaxavis*, *Cathayornis*). The expanded tips extend farther caudally than the xiphial region, whereas these processes do not reach the caudal margin in *Protopteryx* (Zhang and Zhou, 2000). The median trabeculae define a wide “V” with an angle of 72°, similar to *Protopteryx* except in this taxon the distal half is constricted into a short xiphoid process; the median trabeculae are developed into an elongate xiphoid process in most other enantiornithines (e.g. *Longipteryx*, *Concornis*, *Rapaxavis*, *Cathayornis*). Intermediate trabeculae, present in most enantiornithines (e.g. *Longipteryx*, *Concornis*, *Rapaxavis*, *Cathayornis*), are absent, as in *Protopteryx* (Zhang and Zhou, 2000). Costal facets are not present, as in other enantiornithines (Zhou et al., 2005; O'Connor et al., 2011).

Pectoral girdle The scapulae are exposed in lateral view, and only the proximal and distal portions are preserved. The acromion is tapered and laterally hooked as in *Pengornis houi* (Fig. 4); this feature is unique to *Pengornis* among enantiornithines (Zhou et al., 2008) but also present in some Early Cretaceous ornithuromorphs (e. g. *Ambiortus* (Kurochkin, 1985), *Apsaravis* (Norell and Clarke, 2001)). The relative positions of the proximal and distal ends indicate that the shafts of the scapulae are straight and shorter than the humeri in length. The scapulae taper slightly distally, as in *P. houi* holotype (Zhou et al., 2008). The humeral articular facet is round and distinctly concave in the left side, but is intersected by a ridge in the right side, which we suggest is an artifact of preservation.

Only the omal portion of each coracoid is preserved in V 18632. The coracoid is strut-like, with a rounded acrocoracoid process. A procoracoid process is absent, as in *Pengornis houi* (Zhou et al., 2008) and other enantiornithines, with the exception of *Protopteryx*, which bears a small laterally directed process, poorly developed compared to the procoracoid process in ornithuromorphs (Hou, 1997; Zhou and Zhang, 2001, 2005; O'Connor et al., 2010). The scapular articular facet forms a slight convexity below the shoulder end of the coracoid. The coracoids are more complete in *P. houi* holotype, and distally the lateral margin of the corpus is convex (Zhou et al., 2008) as in some enantiornithines (Chiappe and Walker, 2002).

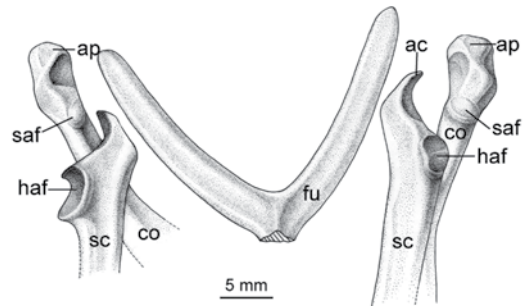


Fig. 4 Camera lucida drawing of the pectoral girdle of the subadult specimen of *Pengornis* sp. (IVPP V 18632)

Abbreviations: ac. acromion 肩峰突; ap. acrocoracoid process 上乌喙骨突; co. coracoid 乌喙骨; fu. furcula 叉骨; haf. humeral articular face 肱骨关节面; saf. scapular articular facet 肩胛骨关节面; sc. scapula 肩胛骨

The furcula of the new specimen differs from that of the holotype of *Pengornis houi*. In V 18632 the furcula is V-shaped, the interclavicular angle is 75° , a value falling within the upper range known for enantiornithines (Chiappe and Walker, 2002); the interclavicular angle appears to be 65° in *P. houi* holotype (Zhou et al., 2008). A hypocleidium was clearly present but is not preserved; a short hypocleidium is preserved in *P. houi* holotype (Zhou et al., 2008), measuring 36.4% the length of the furcular rami. The omal tips are bluntly tapered in both specimens. The clavicular rami are relatively robust and mediolaterally broad in *P. houi* holotype (Zhou et al., 2008), whereas in V 18632 they are straight and slender along their entire lengths. In both specimens, shallow dorsolateral depressions extend along the rami and reach the clavicular symphysis, as in other enantiornithines (Chiappe and Walker, 2002).

Forelimb The left forelimb of V 18632 is more complete and articulated than that of *Pengornis houi* V 15336. The forelimb to hindlimb length ratio is 1.26 (humerus + ulna + carpometacarpus / femur + tibiotarsus + metatarsal III), compared to 1.35 in *Pengornis houi* (Zhou et al., 2008).

The nearly completely preserved humeri in the new specimen are quite different from those of *Pengornis houi* V 15336. The humeri, both exposed in caudal view, are slightly shorter than the ulna. The humeral head is interpreted as not completely ossified, with a flat profile in dorsal view, differing from the more globose condition in *P. houi* holotype (Zhou et al., 2008). However, V 18632 still differs from other enantiornithines in which the middle part of the profile of the humeral head is more or less concave (Chiappe and Walker, 2002). The humerus of V 18632 also differs from the holotype of *P. houi* in having a shallower capital incision and a relatively weaker ventral tubercle. A pneumatic fossa is absent in both *P. houi* holotype (Zhou et al., 2008) and V 18632. The dorsally projecting deltopectoral crest is weaker and narrower in V 18632 than in *P. houi* holotype (Zhou et al., 2008), being less than 1/3 as wide as the humeral shaft rather than approximately equal in width to the shaft as in *P. houi* holotype (Zhou et al., 2008). The crest extends for approximately 1/3 the length of the humerus in V 18632. The distal angle of the deltopectoral crest is less rounded compared to *P. houi* holotype (Zhou et al., 2008). The distal part of the humerus angles ventrally as in *P. houi* holotype, but the olecranon fossa is weaker in V 18632 than in *P. houi* holotype (Zhou et al., 2008).

The ulna is bowed along the proximal 2/3 of its length, but the radius shaft is straight. The two bones are approximately the same length. The ulna is robust and broader than the radius, the ulnar-shaft/radial-shaft mid-shaft width ratio being approximately 1.3 in V 18632 and 1.7 in *P. houi* holotype (Zhou et al., 2008).

In V 18632 the ulnare is heart-shaped and shows little differentiation into rami, but in *P. houi* holotype this bone is differentiated into dorsal and ventral rami (Zhou et al., 2008). A crushed bone between the left radius and semilunate carpal of V 18632 is interpreted as the radiale. In V 18632 the metacarpals are entirely unfused both proximally and distally; the semilunate carpal is fused to the major metacarpal although the suture remains distinct. In *P. houi* V 15336 the proximal ends of the major and minor metacarpals are well fused with the

semilunate carpal (Zhou et al., 2008).

The left manus is completely preserved, and generally similar in morphology to that of *Eoenantiornis* (Zhou et al., 2005), with nearly equal proportions between the length of the carpometacarpus and ulna.

In V 18632 and *Eoenantiornis*, the carpometacarpus is short, being half the length of the ulna as in *Eoenantiornis* (Zhou et al., 2005), whereas the ratios are all more than 60% in *Confuciusornis* (Chiappe et al., 1999), *Cathayornis* (Zhou et al., 1992), *Eocathayornis* (Zhou, 2002), and *Longipteryx* (Zhang et al., 2001) (based on the ratio of the combined length of the semilunate and major metacarpal to the length of the ulna shaft). The alular metacarpal is short and trapezoid, measuring 21% the length of the major metacarpal (approximately 26.7% in *Eoenantiornis*). The major metacarpal is straight and robust. The minor metacarpal is bowed, and more slender than the major metacarpal. It extends significantly farther distally than the major metacarpal as in *P. houi* holotype and other enantiornithines, and has more expanded proximal and distal ends than *P. houi* holotype (Zhou et al., 2008). The intermetacarpal space extends from the proximal 1/3 of the major metacarpal to the distal end.

Unlike the holotype of *Pengornis houi*, V 18632 preserves completely articulated manual phalanges in the left side. The phalangeal formula is 2-3-2 as in other ornithothoracines (Wang et al., 2010). The first phalanx of the alular digit is slender and relatively short, terminating far proximal to the distal end of the major metacarpal, but the unguis phalanx is the largest in the hand. The alular digit is slightly more than half the length of the major carpometacarpus with a relatively large unguis on the alular digit, as in *Eoenantiornis* (Zhou et al., 2005) and *Longipteryx* (Zhang et al., 2001). The first phalanx of the major digit is subtriangular, tapering slightly distally, as in *P. houi* holotype, but differs in that it is slightly medially constricted at about the proximal point 1/3. The reduced second phalanx is shorter and more slender than the first, as in most enantiornithines with the exception of *Protopteryx* (Zhang and Zhou, 2000). The unguis phalanx, preserving its horny sheath, is slightly smaller than the alular unguis. The presence of two phalanges in the minor digit confirms the hypothesis based on the holotype of *P. houi* that this digit had more than one phalanx (Zhou et al., 2008). The first phalanx tapers sharply along the distal 2/3 of its length; the second phalanx, preserved in articulation, is reduced to a small nubbin of bone.

Pelvic girdle V 18632 preserves nearly complete ilia, pubes, and ischia (Fig. 5); the bones are unfused. The pubes are retroverted and nearly the same length as the femur (the proximal portion is not preserved in *P. houi* V 15336). The pubes



Fig. 5 Photo of the sacropelvic area of the subadult specimen of *Pengornis* sp. (IVPP V 18632)

are not in contact distally and overlap and poor preservation prevent determining if a pubic symphysis and or boot, like that of *P. houi* holotype, was present. Proximally, the iliac and pubic pedicels of the ischium are short and weakly separated. The ischium is $3/4$ the length of the pubis; an obtuse, distally located dorsal process appears present on the right ischium, extending along the distal $2/5$ of the bone. Although poorly preserved, this process more closely resembles that of *Confuciusornis* and ornithuromorphs (e.g. *Yixianornis*) (Chiappe et al., 1999; Zhou and Zhang, 2001) than it does the proximally located, strap-like process of most enantiornithines (Chiappe and Walker, 2002). The left ischium preserves a large, blunt, proximodistally elongate oval tubercle on the dorsal surface at approximately the midlength of the bone.

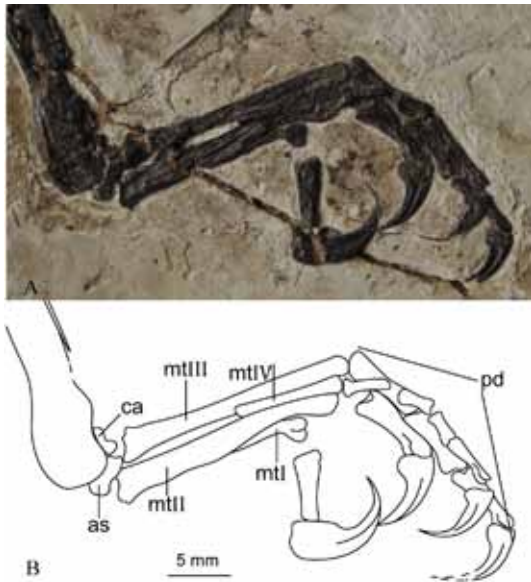


Fig. 6 Photo (A) and camera lucida drawing (B) of the right pes of the subadult specimen of *Pengornis* sp. (IVPP V 18632)

For abbreviations see Fig. 2

medial condyle seems equal to the lateral one in width. The fibula is triangular and elongate; it tapers distally, approaching the ankle joint as in *P. houi* V 15336.

No distal tarsals are preserved in V 18632. Metatarsals II-IV are entirely unfused to each other in V 18632, while they are fused proximally in *P. houi* holotype (Zhou et al., 2008). The J-shaped metatarsal I is preserved pressed to the medial surface of the distal end of metatarsal II, not reaching the proximal margin of the trochlea. The articular facet for the first phalanx of the hallux is caudally directed, opposite to the orientation of other digits, so that the hallux was fully reversed. Metatarsal I is $1/3$ length of metatarsal II. Metatarsals II-IV are straight throughout their length. The tubercle for the attachment of the m. tibialis cranialis on metatarsal II is absent in V 18632 but developed in *P. houi* holotype (Zhou et al., 2008). The

Hindlimb The hindlimb is more completely preserved in V 18632 than in the holotype of *Pengornis houi*. The right hindlimb of V 18632 is missing only the proximal end of metatarsal IV (Fig. 6) and the entire left pes.

The femur is slightly craniocaudally bowed and measures 96% of the length of the tibia, as in *P. houi* holotype (Zhou et al., 2008). The two proximal tarsals are completely free from the tibia and each other, while they appear completely fused to the distal end of the tibia in *P. houi* holotype (Zhou et al., 2008). Proximally no cnemial crest is observed, typical of most enantiornithines. The calcaneum is rectangular and narrow. The astragalus is much larger than the calcaneum and bears an ascending process. The poorly preserved

distal fragment of the right metatarsal IV is disarticulated and displaced to lie between metatarsals II and III. At least distally, metatarsal IV is narrower than metatarsals II and III as in *P. houi* (Zhou et al., 2008) and other enantiornithines (Chiappe and Walker, 2002). As in most enantiornithines, metatarsal III extends farther distally than metatarsal IV, which in turn extends farther distally than metatarsal II. The left metatarsus preserves a bone that we tentatively identify as metatarsal V, although this element has never been preserved in any other enantiornithine (O'Connor et al., 2009). This bone, situated near the proximal tarsals, is short, approximately 17.5% of the length of metatarsal II, and very thin (Fig. 7). Alternatively, this may be the transverse process of an underlying caudal vertebra.

The pedal digits are articulated and completely preserved in the right foot of V 18632. Digit III is the longest, and digit IV is slightly longer than digit II. The first phalanx of digit II is overlapped by digit IV, but the positions of the distal end of metatarsal II and the proximal end of the second phalanx of digit II show that the first phalanx is significantly shorter than the second as in *P. houi* holotype (Zhou et al., 2008). In digit III, the first phalanx is slightly longer than either the second or the third, which are approximately equal in length although the third phalanx is more slender. The phalanges of digit IV are much shorter and more slender than those of the other pedal digits, with the first and fourth phalanges approximately equal in length and longer than the second and third phalanges. All of the pedal unguals are robust and strongly curved. The unguals of II-IV digits are subequal and much smaller than the hallucal claw. The digit II ungual is larger than that of digits III and IV, which are subequal in size.

Plumage No feathers are preserved in the holotype of *Pengornis houi* but V 18632 preserves some faint wing feather impressions and an incomplete single tail feather. The wing feathers are preserved near the bones of the right forelimb as an organic stain with imprints of the rachi. The maximum preserved length of the wing feathers is 55.42 mm, measured from the second phalanx of the right wing major digit to the distal end of the impression of the feathers. Poor preservation makes it impossible to determine whether or not an alula, or bastard wing, was present. An isolated rectrix without the proximal and distal end is preserved as a carbonized trace directed toward the pygostyle. This presumed tail feather is long and fully pennaceous, having more than 20 parallel barbs that form an angle of approximately 13° with the rachis on both sides.

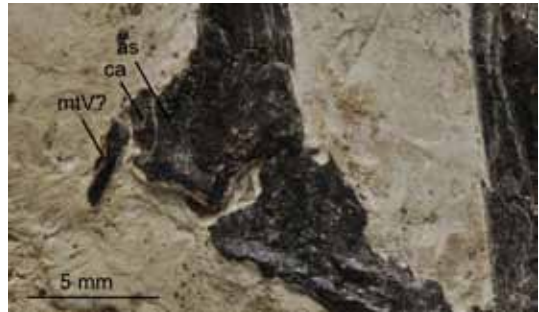


Fig. 7 Photo of the ankle joint showing the tentatively identified metatarsal V of the subadult specimen of *Pengornis* sp. (IVPP V 18632)

For abbreviations see Fig. 2

3 Phylogenetic analysis

A previous phylogenetic analysis by Zhou et al. (2008) placed *Pengornis* within Enantiornithes as the basalmost enantiornithine other than *Protopteryx*. A new phylogenetic analysis was conducted using a modified version of the O'Connor and Zhou (2012) dataset, with the new specimen IVPP V 18632 added to the matrix. A total of 61 taxa were evaluated for 245 characters using TNT (Goloboff et al., 2008). A heuristic search was performed, with 1000 replications, saving 5 trees per replication, followed by another round of TBR branch swapping. The heuristic search returned 155 most parsimonious trees (MPTs) of 856 steps; the second round of TBR branch swapping returned 2160 MPTs of 855 steps. Absolute Bremer support values were calculated and are indicated in the strict consensus tree (Fig. 8A). A reduced consensus tree was also generated, pruning the fragmentary taxon *Otogornis* (Fig. 8B).

The results of the phylogenetic analysis are weakly supported, as in the O'Connor and Zhou (2012) analysis, as indicated from the low values of the Consistency Index (0.381) and Retention Index value (0.663), and the low Bremer support values (Fig. 8).

In the strict consensus tree, Enantiornithes is less resolved than in the O'Connor and Zhou (2012) analysis; a *Boluochia* + *Longipteryx* clade is supported here, as in the previous analysis (O'Connor and Zhou, 2012). In the reduced consensus tree with *Otogornis* removed, Enantiornithes is well resolved and resembles previous results (O'Connor and Zhou, 2012) with two major exceptions: the basal *Elsornis* + *Shenqiornis* clade is no longer supported and *Shenqiornis* is resolved with *Vescornis* in a more derived clade; and *Rapaxavis* and *Iberomesornis* hold relatively more basal positions.

The strict consensus tree resolves V 18632 and *Pengornis houi* as a clade, supporting the hypothesis that V 18632 is referable to *Pengornis*. Although the absolute Bremer support value is extremely low (1 for this node), there are several unambiguous synapomorphies that support this clade: premaxillae unfused (character 1:0); cranial and caudal surfaces of cervical vertebrae heterocoelous (character 51:2); tip of scapula acromion process laterally hooked (character 100:1); and intermetacarpal space wide (character 164:1).

Ornithuromorpha is well resolved in the strict consensus tree as in the previous analysis (O'Connor and Zhou, 2012), but different from the latter in the position of basal taxa: *Gansus*, *Apsaravis* and *Ambiortus* are resolved as basal taxa, while they are more derived in the 2012 analysis; the basal taxa *Patagopteryx*, *Schizooura*, *Vorona*, *Zhongjianornis* and *Chaoyangia* in the 2012 analysis are resolved in a more derived clade in this analysis.

4 Discussion

The new specimen IVPP V 18632 shares several features with *Pengornis houi* that,

based on detailed anatomical comparisons, suggest it represents a new species of *Pengornis*. V 18632 shares with the holotype of *P. houi* (IVPP V 15336)(Zhou et al., 2008) the following diagnostic features: entirely unfused and relatively short premaxillae; numerous small peg-like teeth; and a hooked scapular acromions. The two specimens also have many other features in common, including: cranially heterocoelic vertebrae; fibula approaching tarsal joint; metatarsal III extending farther distally than metatarsal IV, which extends farther distally than metatarsal II; and femur-to-tibia length ratio of 0.92.

The femur of the new specimen is 72.5% as long as that of *P. houi* holotype (Zhou et al., 2008). Apart from its smaller size, V 18632 also displays several morphological features indicating subadult status, such as the porous and coarse articular surfaces of long bones (e.g., humerus, ulna, femur, and tibia)(Horner, 1997; Sanz et al., 1997), and absent or incomplete fusion in compound bones, which are fused in the holotype of *P. houi* (Zhou et al., 2008). The metacarpals are entirely unfused, rather than fused proximally as in the adult specimen; the semilunate carpal is only partially fused to the major metacarpal, retaining a distinct suture, rather than well fused with the major and minor metacarpals. The sacrals are also separated by distinct sutures, rather than completely fused into a synsacrum, and several spinous processes are still visible in the pygostyle. The calcaneum and astragalus are unfused, rather than fused with the tibia, and metatarsals II-IV are unfused, rather than fused proximally.

Apart from the differences that can be easily explained as the result of ontogenetic differences or preservational bias between V 18632 and the holotype of *P. houi* (Zhou et al., 2008), there are also substantial morphological differences indicating the new specimen cannot be referred to *P. houi*, but represents a new species of *Pengornis*. In V 18632, the nasal process of maxilla is much more delicate than that in *P. houi* V 15336, and the jugal process of the maxilla is pointed rather than rodlike in *P. houi* V 15336; the furcula has slender clavicular rami with an interclavicular angle of 75° , rather than the more robust rami with an interclavicular angle of 65° in *P. houi* V 15336; the humeral head is flat, rather than globose as in *P. houi* V 15336; the deltopectoral crest of the humerus is weaker and narrower than in *P. houi* V 15336, being less than 1/3 as wide as the humeral shaft rather than approximately equal in width to the shaft in *P. houi* V 15336; and the pubis is straight, rather than recurved in *P. houi* V 15336. Based on the shared features but substantial differences between V 18632 and the holotype of *P. houi*, and considering the subadult status of V 18632, we refer the new specimen to a new indeterminate species of *Pengornis*.

V 18632 reveals new information regarding the anatomy and life habits of *Pengornis*. The new specimen displays primitive features of the sternum and forelimb that were previously unknown for *Pengornis*.

The sternal morphology preserved in V 18632 contributes information that clarifies evolutionary trends in early birds. The complexity of the sternum increases from basal to more derived taxa (Fig. 9) both throughout Aves and within Enantiornithes and Ornithuromorpha. No sternum is preserved in *Archaeopteryx* (Elzanowski, 2002), *Sapeornis* (Zhou and Zhang,

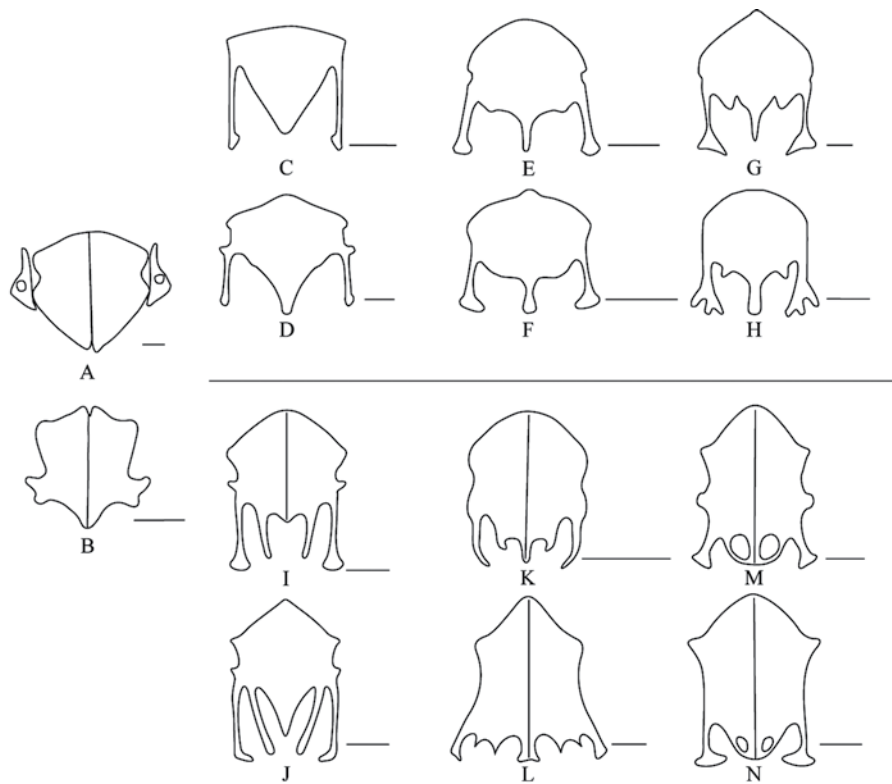


Fig. 9 Sterna of various Mesozoic birds

A. *Jeholornis prima*; B. *Confuciusornis sanctus*; C. IVPP V 18632; D. *Protopteryx fengningensis*; E. *Longipteryx chaoyangensis*; F. *Eocathayornis walkeri*; G. *Cathayornis yandica*; H. *Longirostravis hani*; I. *Archaeorhynchus spathula*; J. FRDC-05-CM-02; K. *Hongshanornis longicresta*; L. *Jianchangornis microdonta*; M. *Yixianornis grabaui*; N. *Yanornis martini*. Scale bar: 1 cm

2002), or *Zhongornis* (Gao et al., 2008). The sternum in *Confuciusornis* and *Jeholornis* is formed from two simple sternal plates with no caudal trabeculae present, indicating the primitive condition (Fig. 9A, B). The sternum in Ornithothoraces (which includes the clades Enantiornithes and Ornithuromorpha) is more complex, possessing caudally directed processes (Zheng et al., 2012).

In Enantiornithes, the lateral, intermediate and median trabeculae appear at different stages. The sternum of *Pengornis*, with its slender lateral trabeculae and V-shaped caudal margin, is fairly simple compared to other enantiornithines except for *Protopteryx*, both taxa lacking intermediate trabeculae and a xiphoid process (Fig. 9C, D), but more complex than in the basal birds such as *Jeholornis* (Zhou and Zhang, 2003) and *Confuciusornis* (Chiappe et al., 1999) which do not possess elongate caudal trabeculae fused to the sternum. In more derived enantiornithines, intermediate trabeculae are present and the distal ends of the lateral trabeculae are remarkably expanded (e.g. *Longipteryx*, *Eocathayornis*, *Bohaiornis*, and *Cathayornis*) (Fig. 9E–G). The intermediate trabeculae range from very slight (e.g. *Longipteryx*) to short

but distinct (e.g. *Dapingfangornis*). In some taxa the distal ends of the lateral trabeculae have complex morphologies (strongly forked in *Longirostravis* (Hou et al., 2004) and *Rapaxavis* (Morschhauser et al., 2009))(Fig. 9H). The primitive sternum in basal birds consists of simple plates; in basal enantiornithines lateral trabeculae and median trabeculae appear, followed by intermediate trabeculae in more derived enantiornithines, so that the sternum becomes progressively more complex within Enantiornithes.

In Ornithuromorpha, both lateral and intermediate trabeculae appear simultaneously and much better developed. Deep caudal incisions similar to those present in enantiornithines are also present in the basal *Archaeorhynchus* (Zhou et al., 2013) and FRDC-05-CM-02 (You et al., 2010)(Fig. 9I, J), as a primitive feature of the ornithuromorph sternum; they differ from the enantiornithines in that the intermediate trabeculae are as long as the lateral trabeculae in Ornithuromorpha (they are much shorter in enantiornithines), and thus two deep pairs of caudal incisions are present (single pair in Enantiornithes). The sternum of *Archaeorhynchus* and FRDC-05-CM-02 are reminiscent of that of *Protopteryx* and V 18632 in the slender lateral trabeculae and V-shaped caudal margin, but the enantiornithines lack the intermediate trabeculae. The sternum is not craniocaudally elongated in basal taxa (Zhou et al., 2013). In taxa more derived than *Archaeorhynchus*, such as hongshanornithids and *Jianchangornis* (Fig. 9K, L), the imperforate portion of the sternum is craniocaudally elongated, and the lateral and intermediate trabeculae form a much shorter contribution to the overall length of the sternum (Zhou et al., 2013). In more derived taxa as *Yixianornis* and *Yanornis* (Fig. 9M, N), the distal ends of the lateral trabeculae are expanded and the intermediate trabeculae contact the median trabeculae to enclose a pair of caudal fenestrae (Zhou et al., 2013). The sterna of basal Ornithuromorpha and basal Enantiornithes bear a resemblance that fades in more derived taxa, suggesting different evolutionary trajectories in sternal evolution in Enantiornithes and Ornithuromorpha.

Features of the hindlimb suggest *Pengornis* most likely was arboreal, but shows a more generalized morphology compared to more derived enantiornithines. The length of the metatarsus is only 21.4% of the total length of the hindlimb, which is indicative of arboreal habits (Hopson, 2001). The pedal unguis are strongly curved, unsuitable for cursorial locomotion, and the unguis of the reversed hallux is particularly well developed. However, the toe proportions in V 18632 are less conclusive and are more generalist in morphology, similar to basal birds such as *Confuciusornis* (Hopson, 2001). Although the second phalanx of digit II is significantly longer than the first phalanx, the proportions of the load bearing digit III (III-1: 35.4%; III-2: 31.3%; III-3: 33.3%) fall between the clusters of clearly terrestrial and clearly arboreal taxa (Hopson, 2001). The morphology of the distal tarsometatarsus is also not indicative of a highly arboreal taxon; metatarsal III extends farther than metatarsals II and IV, whereas in modern arboreal birds the trochlea of metatarsals ends at the same level (Zhou, 1995). However, most enantiornithines lack this latter specialization, despite inferences they are arboreal. The generalist morphology of the foot reveals that enantiornithines became

increasingly better adapted for an arboreal environment as they became more derived. *Boluochia* and *Longipteryx* have subequal metatarsals II-IV (O'Connor et al., 2011) and *Rapaxavis* shows distally elongated phalanges in all pedal digits (Morschhauser et al., 2009).

Acknowledgements We thank Li Yutong for preparing the specimen, Zhang Jie for taking photographs, and Shi Aijuan for help with the illustrations. We are grateful to Corwin Sullivan for his comments and suggestions on an earlier version of the manuscript. We also thank Zhang Jiangyong and Han Fenglu for discussion and assistance. This study was supported by the National Basic Research Program of China (973 Program, 2012CB821906), the National Natural Science Foundation of China (41172020) and the Chinese Academy of Sciences.

鹏鸟(*Pengornis*)—新材料及其对反鸟特征演化的指示意义

胡 晗^{1,2} 周忠和¹ 邹晶梅¹

(1 中国科学院古脊椎动物与古人类研究所, 中国科学院脊椎动物演化与人类起源重点实验室 北京 100044)

(2 中国科学院大学 北京 100049)

摘要: 鹏鸟(*Pengornis*)是早白垩世已知体型最大的反鸟类, 其骨骼兼有反鸟类和今鸟类的特征。报道了辽西九佛堂组新发现的一件鹏鸟的亚成年个体标本, 代表了该属鸟类除侯氏鹏鸟(*Pengornis houi*)正型标本外的已知第二件标本, 暂归入鹏鸟未定种(*Pengornis* sp.)。该标本头骨与头后骨骼近乎完整保存, 并附有羽毛印痕, 仅缺失部分右前肢和部分左后肢。新标本首次提供了鹏鸟胸骨与基干反鸟类原羽鸟(*Protopteryx*)及基干今鸟类古喙鸟(*Archaeorhynchus*)相似的形态特征, 肯定了鹏鸟的基干位置, 并讨论了其在鸟类胸骨演化中的意义。新标本对前肢和后肢(特别是脚趾)等的许多特征也有补充, 表明其应当属于树栖生活的鸟类。

关键词: 辽西, 早白垩世, 九佛堂组, 反鸟类, 鹏鸟

中图法分类号: Q915.865 文献标识码: A 文章编号: 1000-3118(2014)01-0077-21

References

- Baumel J J, Witmer L M, 1993. Osteologia. In: Baumel J J, King A S, Breazile J E et al. eds. Handbook of Avian Anatomy: Nomina Anatomica Avium. 2nd ed. Cambridge, UK: Nuttall Ornithological Club. 45-132
- Benton M J, Zhou Z H, Orr P J et al., 2008. The remarkable fossils from the Early Cretaceous Jehol Biota of China and how they have changed our knowledge. Proc Geol Assoc, 119: 209-228
- Chiappe L M, Ji S A, Ji Q et al., 1999. Anatomy and systematics of the Confuciusornithidae (Aves) from the late Mesozoic of northeastern China. Bull Am Mus, 242: 1-89
- Chiappe L M, Walker C A, 2002. Skeletal morphology and systematics of the Cretaceous Euenantiornithes (Ornithothoraces: Enantiornithes). In: Chiappe L M, Witmer L M eds. Mesozoic Birds: Above the Heads of Dinosaurs. Berkley:

- University of California Press. 240–267
- Elzanowski A, 2002. Archaeopterygidae (Upper Jurassic of Germany). In: Chiappe L M, Witmer L M eds. Mesozoic Birds: Above the Heads of Dinosaurs. Berkeley: University of California Press. 129–159
- Gao C L, Chiappe L M, Meng Q J et al., 2008. A new basal lineage of Early Cretaceous birds from China and its implications on the evolution of the avian tail. *Palaeontology*, 51(4): 775–791
- Goloboff P A, Farris J S, Nixon K C, 2008. TNT, a free program for phylogenetic analysis. *Cladistics*, 24: 774–786
- He H Y, Wang X L, Zhou Z H et al., 2004. Timing of the Jiufotang Formation (Jehol Group) in Liaoning, northeastern China, and its implications. *Geophys Res Lett*, 31: L12605
- Hopson J A, 2001. Ecomorphology of avian and nonavian theropod phalangeal proportions: implications for the arboreal versus terrestrial origin of bird flight. In: Gauthier J, Gall L F eds. New Perspectives on the Origin and Early Evolution of Birds. New Haven: Peabody Museum of Natural History Press. 211–235
- Horner J R, 1997. Rare preservation of an incompletely ossified fossil embryo. *J Vert Paleont*, 17: 431–434
- Hou L H, 1997. Mesozoic Birds of China. Nantou: Phoenix Valley Provincial Aviary of Taiwan. 116–123
- Hou L H, Martin L D, Zhou Z H et al., 1999. *Archaeopteryx* to opposite birds — missing link from the Mesozoic of China. *Vert Palasiat*, 4(2): 88–95
- Hou L H, Chiappe L M, Zhang F C et al., 2004. New Early Cretaceous fossil from China documents a novel trophic specialization for Mesozoic birds. *Naturwissenschaften*, 91: 22–25
- Kurochkin E, 1985. A true carinate bird from Lower Cretaceous deposits in Mongolia and other evidence of Early Cretaceous birds in Asia. *Cretaceous Res*, 6: 271–278
- Li L, Duan Y, Hu D Y et al., 2006. New eoanantiornithid bird from the Early Cretaceous Jiufotang Formation of western Liaoning, China. *Acta Geol Sin*, 80: 38–41
- Martin L D, Zhou Z H, 1997. *Archaeopteryx*-like skull in enantiornithine bird. *Nature*, 389: 556
- Morschhauser E, Varricchio D J, Gao C L et al., 2009. Anatomy of the Early Cretaceous bird *Rapaxavis pani*, a new species from Liaoning Province, China. *J Vert Paleont*, 29: 545–554
- Norell M A, Clarke J A, 2001. Fossil that fills a critical gap in avian evolution. *Nature*, 409: 181–184
- O'Connor J K, Chiappe L M, 2011. A revision of enantiornithine (Aves: Ornithothoraces) skull morphology. *J Syst Palaeont*, 9(1): 135–157
- O'Connor J K, Chiappe L M, Gao C L et al., 2011. Anatomy of the Early Cretaceous enantiornithine bird *Rapaxavis pani*. *Acta Palaeont Pol*, 56: 463–475
- O'Connor J K, Gao K Q, Chiappe L M, 2010. A new ornithuromorph (Aves: Ornithothoraces) bird from the Jehol Group indicative of higher-level diversity. *J Vert Paleont*, 30: 311–321
- O'Connor J K, Wang X R, Chiappe L M et al., 2009. Phylogenetic support for a specialized clade of Cretaceous enantiornithine birds with information from a new species. *J Vert Paleont*, 29: 188–204
- O'Connor J K, Zhou Z H, 2012. A redescription of *Chaoyangia beishanensis* (Aves) and a comprehensive phylogeny of Mesozoic birds. *J Syst Palaeont*, doi: 10.1080/14772019.2012.690455
- Sanz J L, Bonaparte J F, 1992. A new order of birds (Class Aves) from Lower Cretaceous of Spain. In: Campbell K E ed. Papers in Avian Paleontology, Honoring Pierce Brodkorb, Science Series 36. Los Angeles: Natural History Museum of Los Angeles County Press. 39–40
- Sanz J L, Chiappe L M, Pérez-Moreno B P et al., 1997. A nestling bird from the Early Cretaceous of Spain: implications for

- avian skull and neck evolution. *Science*, 276: 1543-1546
- Sereno P C, 2000. *Iberomesornis romerali* (Aves, Ornithothoraces) reevaluated as an Early Cretaceous enantiornithine. *Neues Jahrb Geol Paläont, Abh*, 215: 365-395
- Sereno P C, Rao C G, Li J J, 2002. *Sinornis santensis* (Aves: Enantiornithes) from the Early Cretaceous of northeastern China. In: Chiappe L M, Witmer L M eds. *Mesozoic Birds: Above the Heads of Dinosaurs*. Berkley: University of California Press. 184-208
- Walker C A, 1981. New subclass of birds from the Cretaceous of South America. *Nature*, 292: 51-53
- Wang X R, O'Connor J K, Zhao B et al., 2010. New species of Enantiornithes (Aves: Ornithothoraces) from the Qiaotou Formation in northern Hebei, China. *Acta Geol Sin*, 84: 247-256
- You H L, Atterholt J, O'Connor J K et al., 2010. A second Cretaceous ornithuromorph bird from the Changma Basin, Gansu Province, northwestern China. *Acta Palaeont Pol*, 55: 617-625
- Zhang F C, Ericson G P, Zhou Z H, 2004. Description of a new enantiornithine bird from the Early Cretaceous of Hebei, northern China. *Can J Earth Sci*, 41: 1097-1107
- Zhang F C, Zhou Z H, 2000. A primitive enantiornithine bird and the origin of feathers. *Science*, 290: 1955-1959
- Zhang F C, Zhou Z H, Hou L H et al., 2001. Early diversification of birds: evidence from a new opposite bird. *Chin Sci Bull*, 46: 945-949
- Zheng X T, Wang X L, O'Connor J M et al., 2012. Insight into the early evolution of the avian sternum from juvenile enantiornithines. *Nature Commun*, 3: 1116
- Zhou S, Zhou Z H, O'Connor J K, 2013. Anatomy of the basal ornithuromorph bird *Archaeorhynchus spathula* from the Early Cretaceous of Liaoning, China. *J Vert Paleont*, 33: 141-152
- Zhou Z H, 1995. Discovery of a new enantiornithine bird from the Early Cretaceous of Liaoning, China. *Vert Palasiat*, 33(2): 99-113
- Zhou Z H, 2002. A new and primitive enantiornithine bird from the Early Cretaceous of China. *J Vert Paleont*, 22: 49-57
- Zhou Z H, Barrett P M, Hilton J, 2003. An exceptionally preserved Lower Cretaceous ecosystem. *Nature*, 421: 807-814
- Zhou Z H, Chiappe L M, Zhang F C, 2005. Anatomy of the Early Cretaceous bird *Eoenantiornis buhleri* (Aves: Enantiornithes) from China. *Can J Earth Sci*, 42: 1331-1338
- Zhou Z H, Clarke J, Zhang F C, 2008. Insight into diversity, body size and morphological evolution from the largest Early Cretaceous enantiornithine bird. *J Anat*, 212: 565-577
- Zhou Z H, Jin F, Zhang J Y, 1992. Preliminary report on a Mesozoic bird from Liaoning, China. *Chin Sci Bull*, 37: 1365-1368
- Zhou Z H, Zhang F C, 2001. Two new ornithurine birds from the Early Cretaceous of western Liaoning, China. *Chin Sci Bull*, 46: 1258-1264
- Zhou Z H, Zhang F C, 2002. Largest bird from the Early Cretaceous and its implications for the earliest avian ecological diversification. *Naturwissenschaften*, 89: 34-38
- Zhou Z H, Zhang F C, 2003. *Jeholornis* compared to *Archaeopteryx*, with a new understanding of the earliest avian evolution. *Naturwissenschaften*, 90: 220-225
- Zhou Z H, Zhang F C, 2005. Discovery of an ornithurine bird and its implication for Early Cretaceous avian radiation. *Proc Nat Acad Sci*, 102: 18998-19002